frontiers | Frontiers in Materials

TYPE Original Research
PUBLISHED 20 July 2023
DOI 10.3389/fmats.2023.1216747

Check for updates

OPEN ACCESS

EDITED BY
Wei Ge,
Zhengzhou University, China

REVIEWED BY
Wei Dongle,
Dalian University of Technology, China
Zhang Lei,
Yellow River Institute of Hydraulic Research, China

*CORRESPONDENCE
Fang Wan,
wanxf1023@163.com

RECEIVED 04 May 2023
ACCEPTED 28 June 2023
PUBLISHED 20 July 2023

CITATION
Chai Q, Huang S, Wan F, Wu F and Feng L (2023), A new experimental method to measure and calculate the tensile strength of concrete.
Front. Mater. 10:1216747.
doi: 10.3389/fmats.2023.1216747

A new experimental method to measure and calculate the tensile strength of concrete

Qihui Chai[1,2], Shasha Huang[1], Fang Wan[1]*, Feng Wu[1] and Lingyun Feng[1]

[1]School of Water Resources, North China University of Water Resources and Electric Power, Zhengzhou, China, [2]Henan Key Laboratory of Water Resources Conservation and Intensive Utilization in the Yellow River Basin, Zhengzhou, China

Introduction: A new method is introduced to test the tensile strength of concrete: the cylinder transverse splitting test. Compared with the cylinder splitting (or Brazilian) test, the cylinder transverse splitting test involves different load positions and offers the advantages of doubling the data volume with the same number of specimens and improving the detection accuracy.

Methods: Finite element analysis software was used to simulate the concrete cylinder transverse splitting test and the stress distribution on the failure surface was determined.

Results and Discussion: The results show that the fracture of a cylinder is mainly determined by tensile stress. The splitting strength of normal concrete and crumb rubber concrete, a new environmentally friendly concrete material that has gathered considerable attention in recent years, was obtained by cylinder transverse and cube splitting tests. The cylinder transverse splitting test data show a stable correlation with the cube splitting test data and well characterize the concrete strength. The relationship between the cylinder nominal transverse splitting strength (f_2) and cube splitting strength (f_1) was established on the basis of linear analysis of the test data: $f_1 = 0.51f_2$. The calculated cube splitting strength is in good agreement with the test values.

KEYWORDS

cylinder transverse splitting method, nominal transverse splitting strength, cube splitting strength, crumb rubber concrete, rubber content

1 Introduction

The tensile strength of concrete is substantially less than its compressive strength. Cracks in concrete easily propagate under tension, which can affect its service life and durability (Bhanja and Sengupta, 2005; Ge et al., 2022). A large number of laboratory studies have evaluated the tensile strength of concrete using three main methods: direct tensile tests; beam flexural tests; and splitting tensile tests (Rashid, et al., 2002; Lu and Li, 2011). Direct tension is theoretically considered to yield a tensile strength similar to the true strength of the concrete under pure uniaxial tension (Wu et al., 2012), but is often difficult to apply owing to the lack of control over the initial crack position, local stress concentrations, and eccentricity strain (Swaddiwudhipong et al., 2003; Zi et al., 2008; Sarfarazi et al., 2018). Furthermore, tensile strength values derived from beam flexural tests tend to be higher than those obtained from direct tensile tests (Raphael, 1984). There are two types of splitting tensile tests listed in GB/T50081-2002. (2002): the cube splitting test (Figure 1A) and the

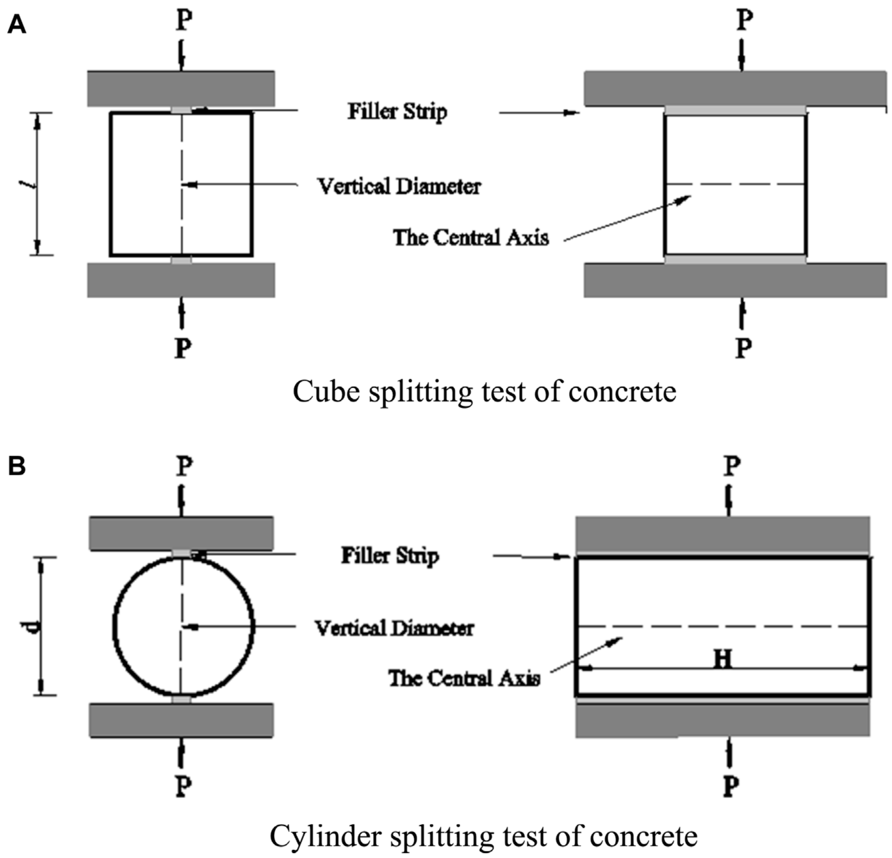

FIGURE 1
Two types of concrete specimen splitting tests: the cube splitting test **(A)** and the cylinder splitting test **(B)**.

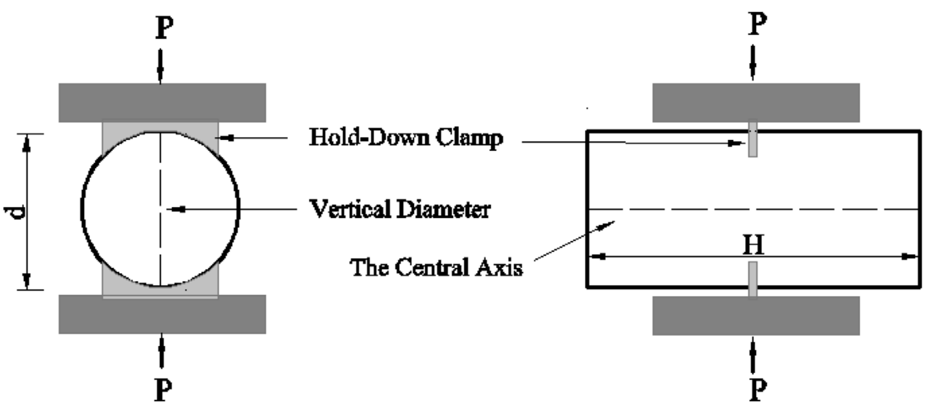

FIGURE 2
Cylinder transverse splitting method.

cylinder splitting (or Brazilian) test (Figure 1B). Previous studies have shown that the tensile strength obtained from cylinder splitting tests are closer to the true tensile strength than flexural tests (Mindess et al., 2002; Wang et al., 2022). The results of cylinder splitting tests have also been shown to provide better tensile strength predications than cube splitting tests (Nilsson, 1961).

TABLE 1 **Cement properties.**

Setting time		Compressive strength		Flexural strength	
Initial	Final	3 days	28 days	3d ays	28 days
169 min	278 min	21.5 MPa	48.3 MPa	5.4 MPa	9.4 MPa

TABLE 2 Aggregate properties.

Material	Size (mm)	Apparent density (kg/m^3)	Mud content (%)	Crushed index (%)	Fineness modulus
coarse aggregates	5~20	2710	0.42	9.3	--
aggregates	0~4.75	2650	1.5	--	2.7

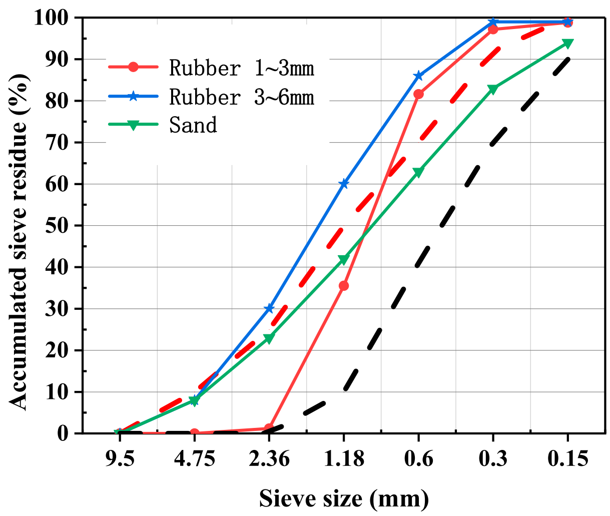

FIGURE 3
Grading curves of sand and rubber particles.

The measurement of concrete strength is important for evaluating the construction quality of completed concrete projects. The drilled-core method is commonly used to detect the concrete structure strength because of its immediacy and reliability (Ge et al., 2020). In this approach, cylindrical specimens with a diameter of 100 mm are drilled from a concrete structure and the compressive strength and splitting strength are tested. The Brazilian test is used to measure the tensile strength of concrete within the core-drilling method. The drilling position and number of samples is stipulated to ensure minimum damage to the concrete structure within the detection range (JGJ/T384-2016, 2016), which can be difficult. The drilled-core method has strict requirements on the height-diameter ratio, perpendicularity, and flatness of the end face of the cylindrical specimen, which increases the difficulty of drilling and specimen processing.

The following limitations are often encountered when using cylinder splitting to measure the tensile strength of concrete following the drilled-core method (JGJ/T384-2016, 2016). 1) Differing from cylindrical specimens made in the laboratory, cylindrical core specimens that are drilled on concrete structures often have variable lengths with uneven end faces. Cylinder core specimens must thus be processed prior to testing with a height-to-diameter ratio of 2. 2) Tensile strength data are often limited because each cylindrical core specimen has only one tensile strength value and concrete structures have a limited amount of available specimen owing to drill core damage (Wang et al., 2023). 3) Specialized skills, tools, and working conditions are required to obtain a complete concrete cylinder core. To improve this situation, Yuan et al. (2006) presented the cylinder transverse splitting method to test the splitting strength of concrete cylinder specimens. Differing from the Brazilian test, the load in the cylinder transverse splitting method is applied across the diameter and perpendicular to the central axis. The direction of the specimen bus bar is thus pulled, which results in splitting tensile failure of the cross-section (Figure 2). The transverse splitting method has the following advantages: 1) increased amount of tensile strength data (a concrete cylinder specimen can be split multiple times); 2) reduced concrete core specimen processing procedure (the end of the concrete core specimen does not need to be cut and leveled); and 3) increased use ratio of the concrete core specimen (a specimen that is shorter than the minimum length specified in JGJ/T384-2016. (2016) can be tested).

Yu et al. (2010) theoretically verified the rationality of multiple transverse cleavage rafting and concluded that higher specimen quantity improves the detection accuracy and reduces the confidence interval difference and upper limit of the variation coefficient. An experimental study by Xiao et al. (2011) showed that the splitting strength (detected by the cylinder transverse splitting method) of a concrete cylinder correlates well with the concrete compressive strength, and that the cylinder transverse splitting method can be used to more accurately and conveniently determine the concrete materiality than traditional core axial compression methods. Yuan et al. (2016) used a finite element model to analyze the rationality of the stress distribution on the transection of cylindrical concrete and found that the tensile failure of the transection depends on the cylinder's axial tensile stress.

TABLE 3 Mixture proportions of NC (kg/m^3).

Mixtures	Water–cement ratio	Water	Cement	Crushed stones	Sand
NC0.74	0.74	195	262.4	1197.3	733.8
NC0.62	0.62	195	312.2	1170.6	717.5
NC0.54	0.54	195	362.1	1143.8	701.1
NC0.42	0.42	195	461.9	1161.6	598.4
NC0.38	0.38	195	511.7	1133.1	583.7
NC0.35	0.35	195	557.14	1107.48	570.52

TABLE 4 Mixture proportions of CRC (kg/m^3).

Mixtures	Rubber content (%)	Water–cement ratio	Water	Cement	Crushed stones	Sand	Rubber
CRC0.74-1	1	0.74	195	262.4	1197.3	726.5	3.00
CRC0.54-1		0.54	195	362.1	1143.8	694.1	2.90
CRC0.42-1		0.42	195	461.9	1161.6	592.4	2.48
CRC0.38-1		0.38	195	511.7	1133.1	577.9	2.42
CRC0.35-1		0.35	195	557.14	1107.48	564.8	2.36
CRC0.74-3	3	0.74	195	262.4	1197.3	711.8	9.00
CRC0.54-3		0.54	195	362.1	1143.8	680	8.71
CRC0.42-3		0.42	195	461.9	1161.6	580	7.43
CRC0.38-3		0.38	195	511.7	1133.1	566.2	7.25
CRC0.35-3		0.35	195	557.14	1107.48	553.4	7.09
CRC0.74-5	5	0.74	195	262.4	1197.3	679.3	15.00
CRC0.54-5		0.54	195	362.1	1143.8	666.1	14.50
CRC0.42-5		0.42	195	461.9	1161.6	568.4	12.40
CRC0.38-5		0.38	195	511.7	1133.1	554.7	12.10
CRC0.35-5		0.35	195	557.14	1107.48	541.92	11.80
CRC0.74-10	10	0.74	195	262.4	1197.3	660.8	30.00
CRC0.54-10		0.54	195	362.1	1143.8	631.1	29.00
CRC0.42-10		0.42	195	461.9	1161.6	538.4	24.80
CRC0.38-10		0.38	195	511.7	1133.1	525.7	24.20
CRC0.35-10		0.35	195	557.14	1107.48	513.3	23.60
CRC0.74-15	15	0.74	195	262.4	1197.3	624.3	45.00
CRC0.54-15		0.54	195	362.1	1143.8	596.1	43.50
CRC0.42-15		0.42	195	461.9	1161.6	508.4	37.20
CRC0.38-15		0.38	195	511.7	1133.1	496.7	36.30
CRC0.35-15		0.35	195	557.14	1107.48	484.7	35.40

TABLE 5 Specimen number and size for each group.

Test	Number	Size
Standard cube splitting strength	3	150 mm × 150 mm × 150 mm
Non-standard cylinder transverse splitting method	3	Ø 100 mm × 200 mm

Although the cylinder transverse splitting method has been shown to be feasible for testing the concrete tensile strength in many aspects (e.g., testing, mathematical statistics, finite element modeling), the cylinder transverse splitting strength is difficult to determine using a reasonable calculation formula. The cylinder transverse splitting strength was previously expressed by the nominal transverse splitting strength, P/A, where P is the failure load and A is the surface area cleavage. In this study, a strong correlation is found between the nominal transverse splitting strength of cylindrical concrete obtained by the cylinder transverse splitting method and the splitting strength of cubic concrete. A calculation formula to test the concrete tensile strength by the cylindrical transverse splitting method is established using the regression of a large number of experimental data. On the basis of previous tests, this study developed an improved specimen clamp for the cylinder transverse splitting method. In addition to normal concrete (NC), crumb rubber concrete (CRC) was also investigated to increase the amount of data and explore a wider range of concrete composition.

CRC is a new environmentally friendly concrete material made by the addition of rubber particles (e.g., crushed automobile tire waste) into ordinary concrete and has broad engineering application prospects (Lin et al., 2023). The rubber particles have a good elasticity, which can alleviate the stress concentration inside the concrete and reduce the probability of primary crack formation and concrete structural damage caused by an external load (Youssf et al., 2023). The addition of rubber particles to NC improves its crack resistance (Li et al., 2021; Elsayed et al., 2022; Feng et al., 2022), impact resistance (Topcu and Avcular, 1997), freeze-thaw durability

FIGURE 4
Cube splitting test.

(Savas et al., 1997; Paine and Dhir, 2002; Khan et al., 2021), abrasion resistance (Hang and Fan, 2011; Sun et al., 2021; Zhang et al., 2023), and reduces its elasticity modulus (Hernandez et al., 2002; Benazzouk et al., 2003; Haldar and Karmakar, 2021). Rubber particles can also reduce the concrete strength (Xu et al., 2020; Xu et al., 2021; Han et al., 2023). Segre et al. (2002) pointed out that zinc stearate tends to reduce the binding force between rubber particles and cement by infrared rays and chemical titration. Although Segre and Jocke (2000) found that rubber particles soaked in saturated NaOH solution for 20 min prior to mixing with the cement slurry improved the compressive strength, splitting strength, and bending strength of rubber cement mortar, they were unable to reach the strength level without the addition of rubber particles.

FIGURE 6
Setup installation.

The CRC tensile strength testing method must be thoroughly investigated to ensure engineering application safety (Adeboje et al., 2020).

2 Materials and methods

2.1 Materials

Ordinary Portland Cement 42.5 was used in this study and its properties are listed in Table 1. The coarse aggregates were limestone gravel and the fine aggregates were natural river sand and rubber particles of 1–3 and 3–6 mm, the latter of which were obtained by crushing scrap tires. The properties of the coarse and fine aggregates are listed in Table 2. The apparent density of the rubber particles is 1119 kg/m^3. The grading curve of the fine aggregates and rubber particles is shown in Figure 3. The indexes of the fine and coarse

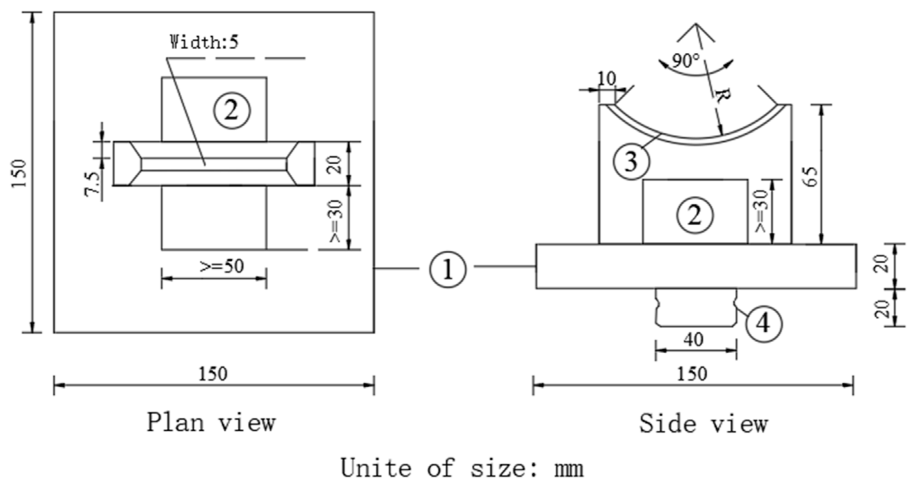

FIGURE 5
Schematic diagram of the test fixture: ① pressing plate; ② stiffening rib; ③ pressure cutter; and ④ connecting bolt.

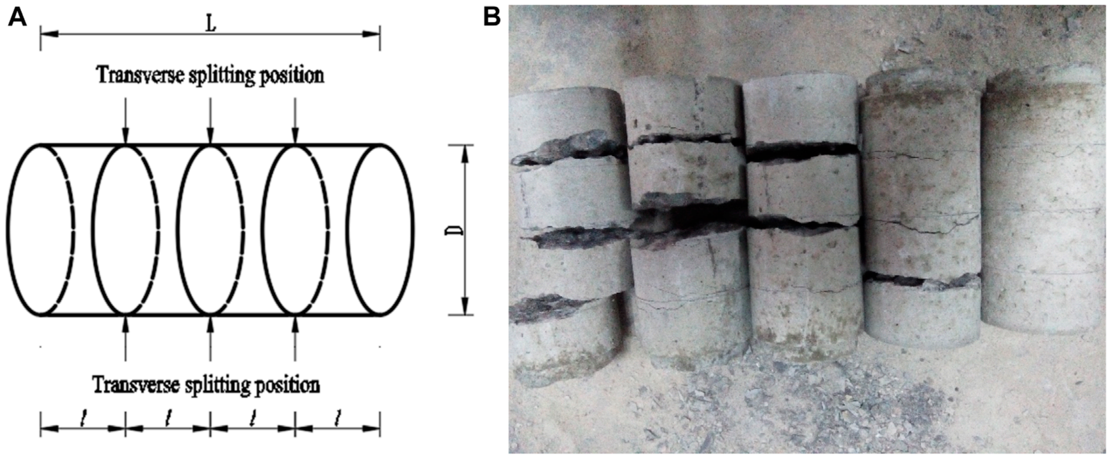

FIGURE 7
Transverse splitting position of cylinder specimen (D = 100 mm, L = 200 mm, l = 50 mm) **(A)**. The cylinder specimen could be uniformly split three times **(B)**.

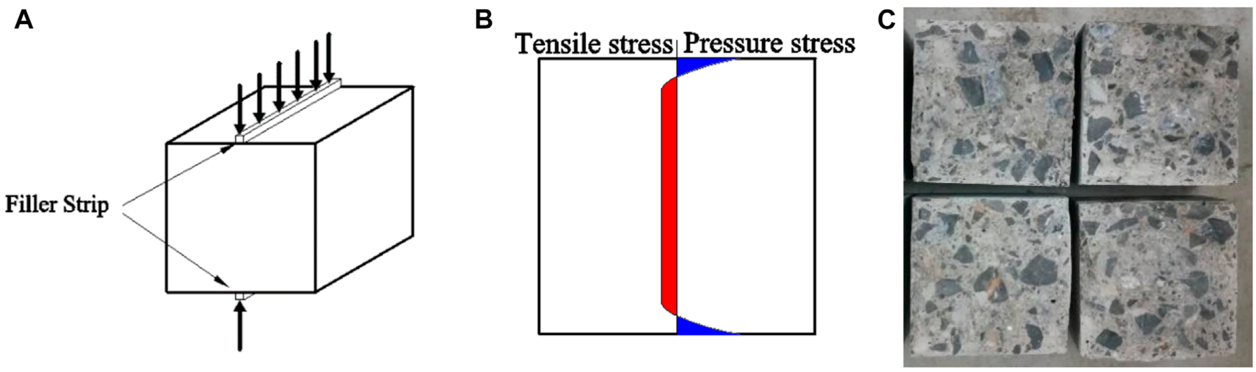

FIGURE 8
In the cube splitting tests, an evenly distributed compression load was applied to the middle of the upper and lower surfaces of the concrete specimen **(A)**. The compression load caused compressive stress in the axial surface of the concrete specimen and uniform tensile stress in most of the middle area **(B)**. The fracture surface exhibited failure under tensile stress **(C)**.

aggregates meet the requirements of GB/T14684-2011. (2011) and GB/T14685-2011. (2011).

2.2 Mixtures

Six water-cement ratios (W/C) were used, as listed in Table 3. The CRC was produced by partially replacing the fine aggregates with rubber particles in volumetric proportions of 1%, 3%, 5%, 10%, and 15% (Table 4). The samples covered a relevant concrete strength range that is commonly used in concrete engineering.

2.3 Specimen preparation

Each mixture proportion contained cubic and cylindrical transverse splitting specimens. The specimens for testing the mechanical properties were prepared based on SL352-2006. (2006) and the number and size are listed in Table 5.

2.4 Test method

2.4.1 Finite element simulations

ANSYS software was used to simulate the transverse splitting tests of the concrete cylinders. The simulations included solid 65 as the concrete material, a sample size of Φ0.1 × 0.1 m, elastic modulus of 30,000 MPa, and Poisson's ratio of 0.2. The constitutive relation adopts the Drucher-Prager model. The failure criterion is an improved William-Warnke five-parameter failure surface, which requires that the following parameters be defined: uniaxial tensile strength; uniaxial compression strength; biaxial compression strength; and uniaxial and biaxial compression strength under a certain confining pressure. Owing to the lack of multi-axis test parameters, ANSYS only requires uniaxial tensile strength

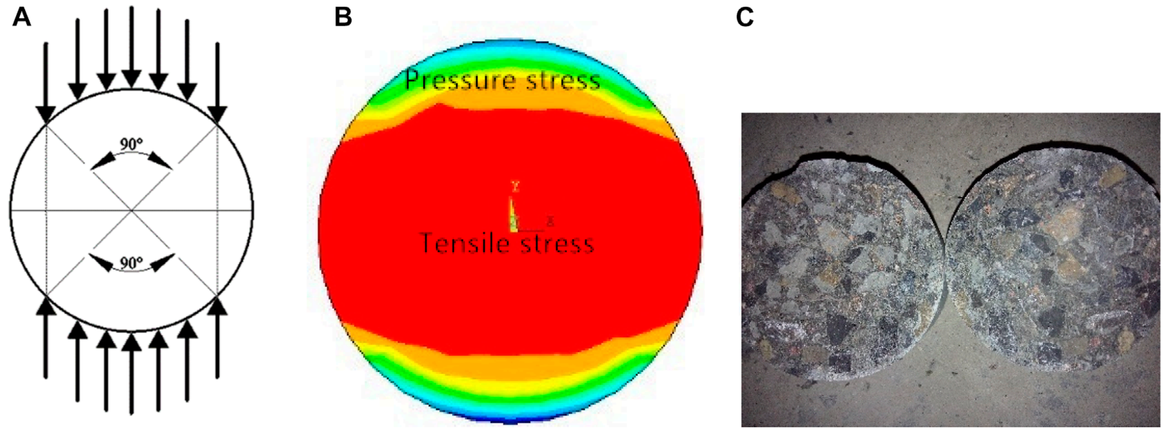

FIGURE 9
In the cylinder transverse splitting tests, the cylinder specimen was uniformly loaded on the cross-sectional curve along the circumference **(A)**. The concrete specimen cross-section was under a state of tension and compression complex stress **(B)**, whereas most of the central area was under a state of tension stress, which influences the splitting failure. The fracture surface performance is consistent with the stress analysis results **(C)**.

and uniaxial compression strength input values, and the other parameters were calculated by the ANSYS default formula. The fracture opening shear transfer coefficient of concrete was 0.3, the fracture closing shear transfer coefficient was 0.9, and the uniaxial tensile strength was 3 MPa. Concrete crushing failure was not considered in the calculation. The remaining concrete parameters were set to the ANSYS default values. The parameters are selected according to the mechanical properties of the most common C30 concrete. The elastic modulus is about 30000 MPa, and the tensile strength is about 3 MPa (1/10 of the compressive strength). The shear stress transfer coefficient of open fissure in concrete is 0.3–0.5, which is 0.3 in this paper. The shear stress transfer coefficient of closed cracks is 0.9–1.0, which is 0.9 in this paper.

2.4.2 Cube splitting tests

Cube splitting tests were performed in accordance with SL352-2006. (2006). The test instrument was a hydraulic universal testing machine with a maximum test force of 2000 kN. The experimental device is shown in Figure 4, which includes a steel square filler strip with a cross-section of 5 × 5 mm and length of 200 mm. To apply a linear uniform load on the concrete surface, the filler strip was placed between the concrete surface and pressure plate (Tang, 1994; Rocco et al., 2000; Olesen et al., 2006). The cube splitting strength of concrete was calculated according to:

$$f_1 = \frac{2P_1}{\pi A_1} = 0.637\frac{P_1}{A_1} \tag{1}$$

where f_1 is the cube splitting strength (MPa), P_1 is the failure load (N), and A_1 is the cross-sectional area (mm^2).

2.4.3 Cylinder transverse splitting method

The setup used in the cylinder transverse splitting test is shown in Figure 5. One of each of the upper and lower pressure plates of the hydraulic servo universal testing machine was used (Figure 6). The test instrument was a hydraulic universal testing machine with a maximum test force of 1000 kN. The contact position with the concrete specimen was an anti-arc pressure cutter (equivalent of a filler strip) and the contact surface was 5-mm wide.

The cylinder transverse splitting test process was as follows. The cylinder specimens were cured in a standard curing room for 28 days and immediately tested after removing the surface moisture. A pencil was used to mark the circumference parallel to the specimen cross-section to determine the splitting position (Figure 7A). The displacement boundary conditions of the cylinder specimens are related closely to the cylinder shape (Jia, 1997; Kanos et al., 2006; Yang and Li, 2002; Zhou et al., 2008; Wu et al., 2021) and the height-diameter ratio is the basic parameter that reflects the cylinder shape characteristics. Yuan et al. (2016) found that the transverse fracture failure load changed little with increasing specimen height when the cylinder height-diameter ratio was greater than or equal to 0.7 and is thus considered stable. The cylinder specimen could therefore be uniformly split three times. The height-diameter ratio was 2 in the first splitting and 1 in the second and third splittings (Figure 7B). A vernier caliper was used to measure the cylinder diameter along the predetermined splitting position. The mean value of three measurements was taken as the effective specimen diameter to calculate the cross-sectional area A_2. The sample was placed between the aligned upper and lower pressure knives according to the predetermined splitting position. The failure load P_2 was recorded at 0.04–0.06 MPa/s.

The cylinder nominal transverse strength of concrete is defined as:

$$f_2 = \frac{P_2}{A_2} \tag{2}$$

where f_2 is the nominal cylinder transverse strength (MPa), P_2 is the failure load (N), and A_2 is the cross-sectional area (mm^2).

10.3389/fmats.2023.1216747

TABLE 6 Test result.

W/C	0.75				0.54			
Particle size and mixing amount of rubber	Cube splitting tensile failure load	Standard deviation	Cylinder transverse splitting tensile failure load	Standard deviation	Cube splitting tensile failure load	Standard deviation	Cylinder transverse splitting tensile failure load	Standard deviation
NC	48.07	10.10	25.24	2.15	90.46	3.48	13.19	9.97
	70.74		31.46		88.42		41.92	
	68.00		27.20		96.61		34.92	
			27.77				41.07	
			27.83				37.75	
			30.89				40.35	
3–6mm, 5%	63.07	6.10	28.65	3.85	93.13	3.67	32.95	4.24
	59.44		37.66		88.00		45.44	
	73.80		27.40		84.18		39.23	
			28.20				33.07	
			25.89				36.49	
			27.86				38.16	
3–6mm, 10%	53.59	6.80	17.53	6.35	85.70	1.05	33.26	4.3
	61.15		38.63		83.17		43.89	
	70.23		25.57		84.81		39.21	
			23.10				31.87	
			26.09				36.86	
			27.95				32.33	
3–6mm, 15%	72.00	8.04	20.79	2.39	82.74	4.31	31.98	2.98
	52.42		28.07		72.78		39.89	
	60.47		23.29		80.80		34.59	
			21.69				32.59	
			24.90				30.68	
			22.61				32.78	
1–3mm, 5%	59.61	4.04	21.08	2.49	83.15	4.46	24.08	4.81

(Continued on the following page)

TABLE 6 (*Continued*) Test result.

W/C	0.75				0.54			
Particle size and mixing amount of rubber	Cube splitting tensile failure load	Standard deviation	Cylinder transverse splitting tensile failure load	Standard deviation	Cube splitting tensile failure load	Standard deviation	Cylinder transverse splitting tensile failure load	Standard deviation
	67.23		28.31		83.15		38.16	
	57.95		27.26		92.61		36.28	
			27.15				37.55	
			27.81				36.57	
			24.81				34.15	
1–3mm, 10%	62.33	4.11	17.15	2.49	78.59	2.30	28.77	2.28
	56.88		24.09		80.16		35.93	
	52.28		24.01		84.05		32.92	
			23.08				35.14	
			24.37				32.56	
			22.50				33.16	
1–3mm, 15%	53.11	1.04	14.29	2.58	83.23	4.43	28.10	1.93
	50.70		18.51		79.14		33.48	
	51.19		22.12		72.48		29.63	
			21.60				32.15	
			19.61				33.28	
			20.34				31.30	
W/C	0.42				0.38			
Particle size and mixing amount of rubber	Split tensile failure load of cube	standard deviation	transverse Split tensile failure load of cylinder	standard deviation	Split tensile failure load of cube	standard deviation	transverse Split tensile failure load of cylinder	standard deviation
NC	102.06	4.92	45.96	3.18	133.99	7.01	48.44	3.87
	108.71		54.59		116.91		59.16	
	114.1		45.65		124.01		52.81	
			47.27				56.8	
			45.42				55.18	
			46.92				49.25	

(Continued on the following page)

10.3389/fmats.2023.1216747

TABLE 6 (*Continued*) Test result.

W/C	0.42				0.38			
Particle size and mixing amount of rubber	Split tensile failure load of cube	standard deviation	transverse Split tensile failure load of cylinder	standard deviation	Split tensile failure load of cube	standard deviation	transverse Split tensile failure load of cylinder	standard deviation
3–6mm, 5%	107.49	4.41	37.58	5.81	122.75	3.22	49.11	2.46
	99.8		56.35		123.21		57	
	110.23		45.94		116.17		52.06	
			43.16				50.41	
			42.02				52.96	
			47.62				51.95	
3–6mm, 10%	106.14	5.73	46.02	5.67	85.70	3.06	43.96	7.39
	101.56		56.98		83.17		66.39	
	92.37		43.34		84.81		50.03	
			44.27				46.49	
			40.51				48.34	
			39.98				47.16	
3–6mm, 15%	80.46	8.04	40.94	6.23	110.43	5.96	38.59	7.63
	96.78		57.3		96.26		61.51	
	98.18		40.64		100.34		45.97	
			41.83				41.26	
			40.65				44.26	
			39.43				40.4	
1–3mm, 5%	109.46	5.42	39.34	5.92	123.14	9.26	51.71	2.71
	106.56		58.04		102.16		58.77	
	96.78		45.68		120.09		51.63	
			42.4				50.61	
			43.09				52.69	
			46.15				51.81	
1–3mm, 10%	98.51	1.91	34.98	4.44	118.06	7.58	42.66	6.21
	100.94		47.76		110.24		61.37	
	103.18		43.88		99.56		47.6	

(Continued on the following page)

TABLE 6 (*Continued*) **Test result.**

W/C	0.42				0.38			
Particle size and mixing amount of rubber	Split tensile failure load of cube	standard deviation	transverse Split tensile failure load of cylinder	standard deviation	Split tensile failure load of cube	standard deviation	transverse Split tensile failure load of cylinder	standard deviation
			45.47				49.68	
			39.7				45.11	
			38.03				44.24	
1–3mm, 15%	102.32	4.92	26.73	5.07	103.98	7.01	34.53	4.56
	90.36		39.35		107.27		47.76	
	95.02		38.2		91.04		40.21	
			40.24				39.05	
			40.42				42.09	
			41.83				46.9	
W/C	**0.35**							
Particle size and mixing amount of rubber	**Split tensile failure load of cube**	**standard deviation**	**transverse Split tensile failure load of cylinder**	**standard deviation**				
NC	133	3.22	51.01	5.03				
	140.19		65.18					
	133.78		62.96					
			58.16					
			60.09					
			53.13					
3–6mm, 5%	137.69	4.55	44.15	6.39				
	129.67		62.93					
	126.98		56.98					
			57.08					
			61.87					
			51.47					
3–6mm, 10%	127.91	20.47	44.13	5.64				
	93.47		62.58					
	142.24		51.13					

(Continued on the following page)

10.3389/fmats.2023.1216747

TABLE 6 (*Continued*) Test result.

W/C	0.35								
Particle size and mixing amount of rubber	Split tensile failure load of cube	standard deviation	transverse Split tensile failure load of cylinder	standard deviation					
			54.33						
			48.66						
			52.04						
3–6mm, 15%	111.45	13.31	42.92	7.71					
	104.12		65.74						
	80.27		46.26						
			44.31						
			46.03						
			50.25						
1–3mm, 5%	126.67	4.88	46.88	3.42					
	131.63		56.21						
	119.72		55.92						
			54.38						
			53.93						
			57.3						
1–3mm, 10%	97.12	12.39	42.91	5.73					
	115.53		57.48						
	127.21		43.65						
			48.19						
			53.14						
			56.14						
1–3mm, 15%	105.45	1.34	40.72	5.01					
	108.37		53.52						
	105.63		44.65						
			44.95						
			40.71						
			51.94						

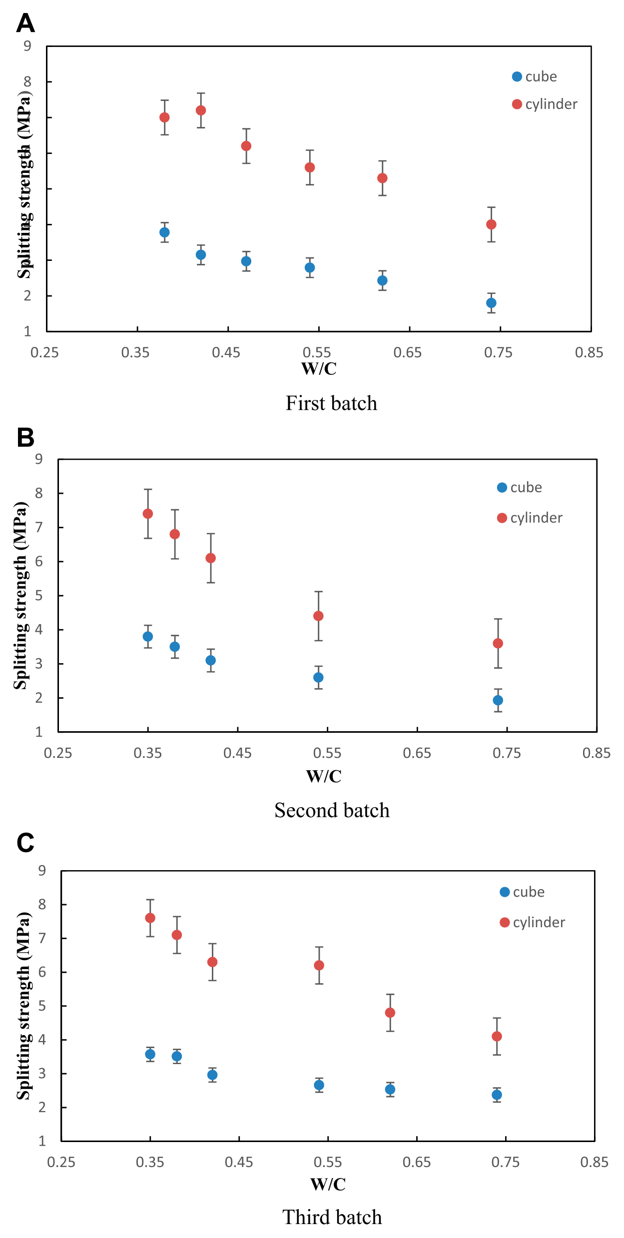

FIGURE 10
Relationship between splitting strength (NC) and W/C: First batch **(A)**; Second batch **(B)**; Third batch **(C)**.

3 Results and discussion

3.1 Comparison of forces

In the cube splitting tests, an evenly distributed compression load was applied to the middle of the upper and lower surfaces of the concrete specimen (Figure 8A). The compression load caused compressive stress in the axial surface of the concrete specimen (same plane as the load) and uniform tensile stress in most of the middle area (Figure 8B). The fracture surface exhibited failure under tensile stress (Figure 8C). The cylinder transverse splitting tests differed in that the cylinder specimen was uniformly loaded on the cross-sectional curve along the circumference (Figure 9A). The load direction was the plumb direction, the same as in the cube splitting tests. The results from the ANSYS stress analysis show that the concrete specimen cross-section was under a state of tension and compression complex stress (Figure 9B), whereas most of the central area was under a state of tension stress, which influences the splitting failure. The fracture surface performance is consistent with the stress analysis results (Figure 9C), which indicates that the cylinder transverse splitting test can be used to effectively measure the concrete splitting strength.

3.2 Comparison of standard deviations

Three batches of cubic and cylindrical specimens of NC were made at different times (in 2011, 2014, and 2017) for the cube and cylinder transverse splitting tests. The standard deviation indicates the degree of data dispersion; smaller standard deviations reflect more concentrated data distributions. The relative precision of the test data can thus be explained by comparing the standard deviations obtained during the cylinder transverse splitting *versus* the cube splitting tensile failure loads. Each group of the second test (in 2014) consisted of three cubic and two cylindrical specimens and thus involved three cubic splitting tensile failure tests and six cylinder transverse splitting failure tests, as shown in Table 6. The standard deviation of the cylinder transverse splitting test results are generally smaller than those obtained from the cube splitting test results. The precision of the concrete tensile strength values obtained by the cylinder transverse splitting test is slightly higher than that of the cube splitting tests.

3.3 NC splitting strength

The cube splitting strength and cylinder nominal transverse splitting strength of the NC show similar negative dependencies with W/C (Figure 10), which is in agreement with the W/C law of Abrams. The cylinder nominal transverse splitting strength is found to be higher than the cube splitting strength for concrete with the same W/C. These results are in agreement with previous studies (Malhotra, 1970; Hang and Fan, 2011) mainly because of the size effect.

3.4 CRC splitting strength

Similar to NC, the cube splitting strength and cylinder nominal transverse splitting strength of CRC decrease with increasing W/C (Figure 11) and show the same trend regardless of the rubber particle size (3–6 or 1–3 mm) or rubber particle content (5%, 10%, or 15%). This regularity shows no correlation with rubber particle size and content. The samples with 1% and 3% rubber particle contents show the same behavior and are not discussed further.

As shown in Figure 12, regardless of rubber particle size (3–6 or 1–3 mm) and W/C (0.35, 0.42, or 0.74), the cube splitting strength and cylinder nominal transverse splitting strength both consistently decrease with increasing rubber particle content. This is mainly

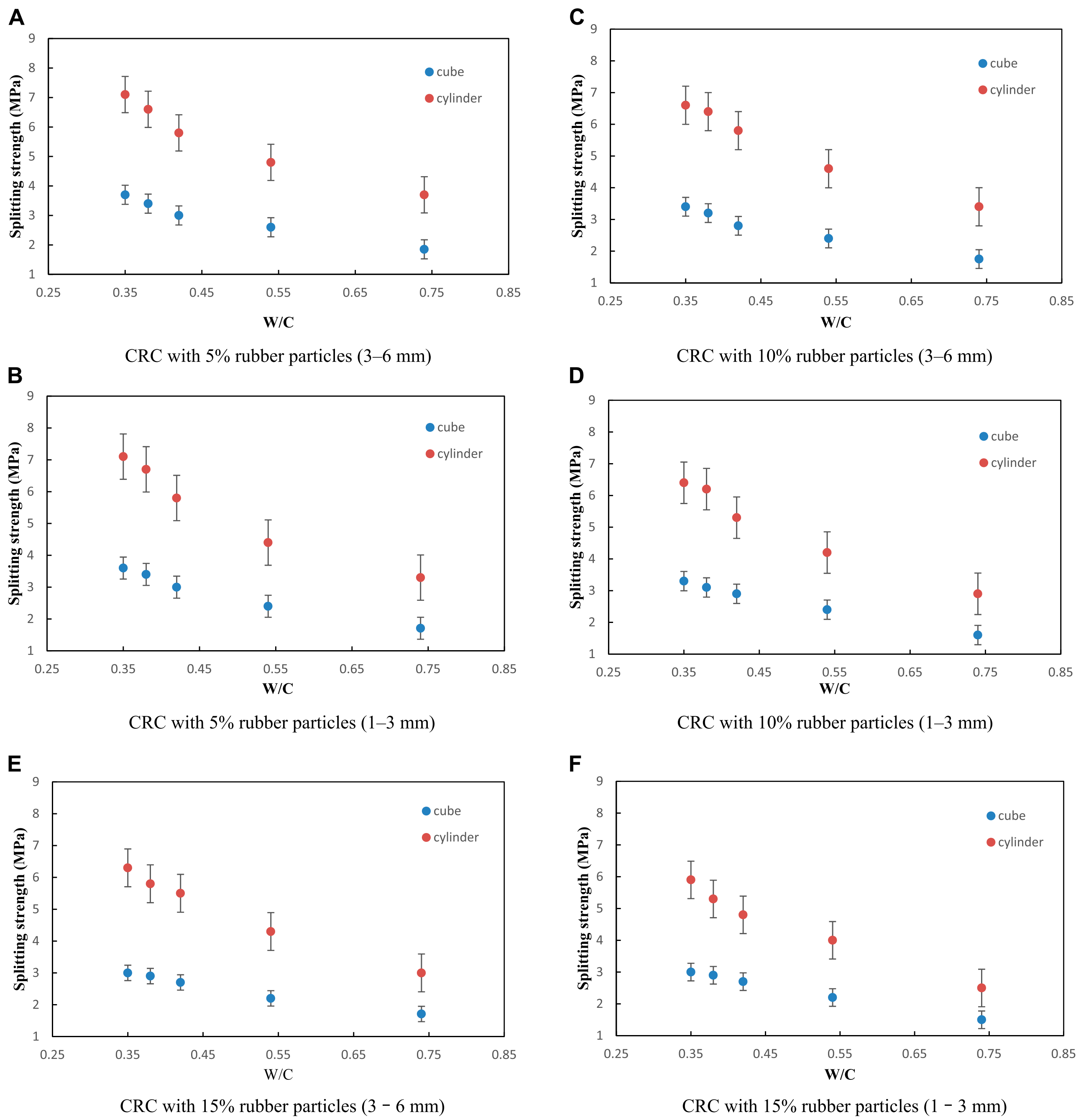

FIGURE 11
Relationship between splitting strength (CRC) and W/C: CRC with 5% rubber particles (3–6 mm) **(A)**; CRC with 5% rubber particles (1–3 mm) **(B)**; CRC with 10% rubber particles (3–6 mm) **(C)**; CRC with 10% rubber particles (1–3 mm) **(D)**; CRC with 15% rubber particles (3–6 mm) **(E)**; CRC with 15% rubber particles (1–3 mm) **(F)**.

because the rubber particle strength is far less than the sand strength, and the bond strength between the rubber and cement is far less than the bond strength between the sand and cement. The samples with 0.38 and 0.54 W/C show the same behavior and are not discussed here. The influence of rubber particle content on concrete strength is similar to previous results (Eldin and Senouci, 1993; Topcu, 1995; Toutanji, 1996; Ali et al., 2000). For the same rubber particle content, the cylinder nominal transverse splitting strength is higher than the cube splitting strength.

On the basis of the above analysis, the cylinder nominal transverse splitting strength can be used to represent the concrete tensile strength, similar to the cube splitting strength.

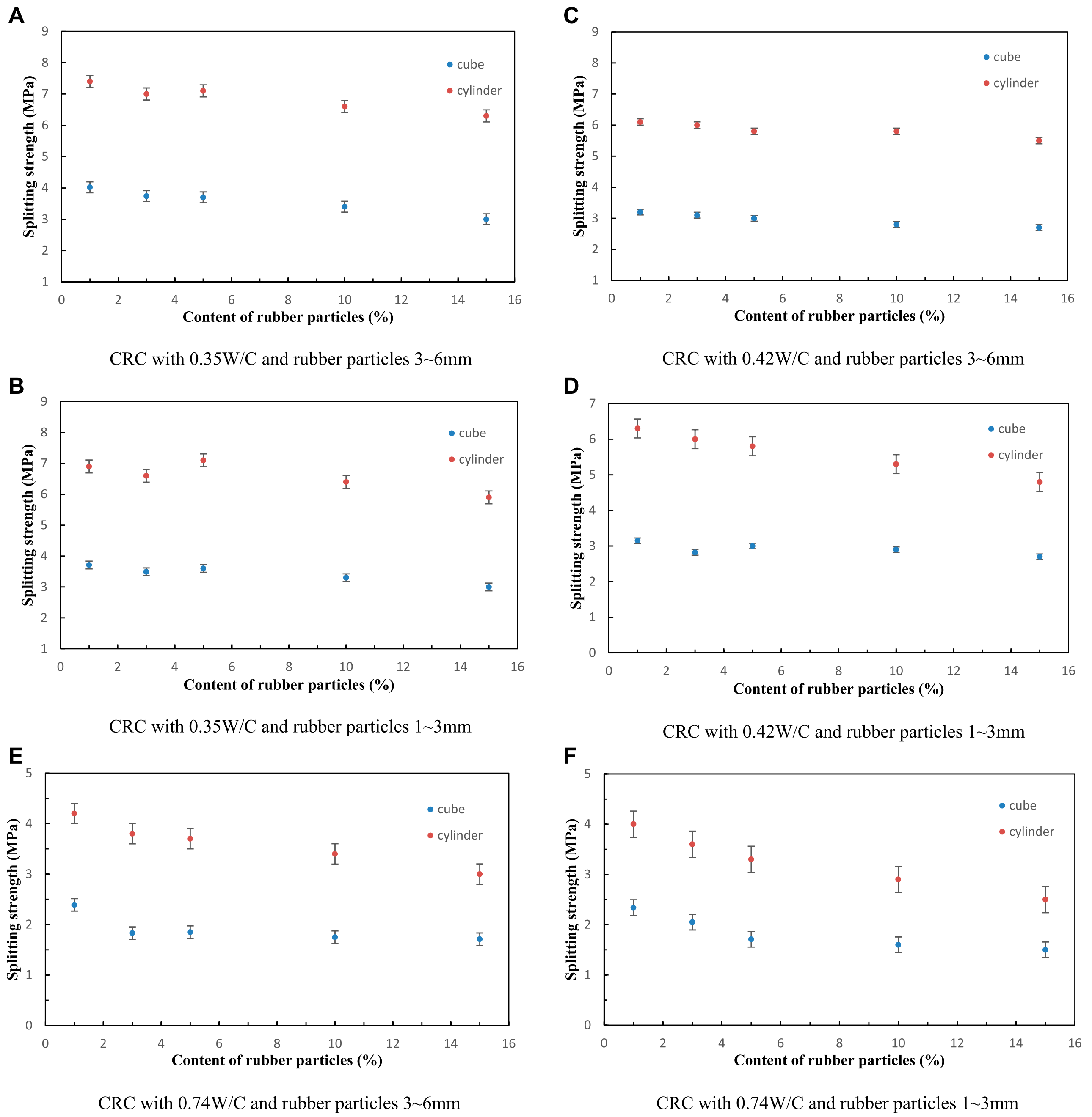

FIGURE 12
Relationship between splitting strength (CRC) and content of rubber particles: CRC with 0.35W/C and rubber particles 3~6 mm **(A)**; CRC with 0.35W/C and rubber particles 1~3 mm **(B)**; CRC with 0.42W/C and rubber particles 3~6 mm **(C)**; CRC with 0.42W/C and rubber particles 1~3 mm **(D)**; CRC with 0.74W/C and rubber particles 3~6 mm **(E)**; CRC with 0.74W/C and rubber particles 1~3 mm **(F)**.

3.5 Relationship between cube and cylinder nominal transverse splitting strength

The cube splitting strength is given in SL352-2006. (2006) as Eq. 1. The concrete splitting surface has a similar stress distribution under the condition of cylinder transverse and cube splitting (Figure 8B; Figure 9B). The cylinder transverse splitting strength is assumed to follow a formula in the same form as the cube splitting strength, namely:

$$f_2' = \gamma \frac{P_2}{A_2} \tag{3}$$

where f_2' is the cylinder transverse splitting strength (MPa) and γ is the coefficient of stress distribution. The results show that an internal relationship exists between the cube and cylinder transverse splitting

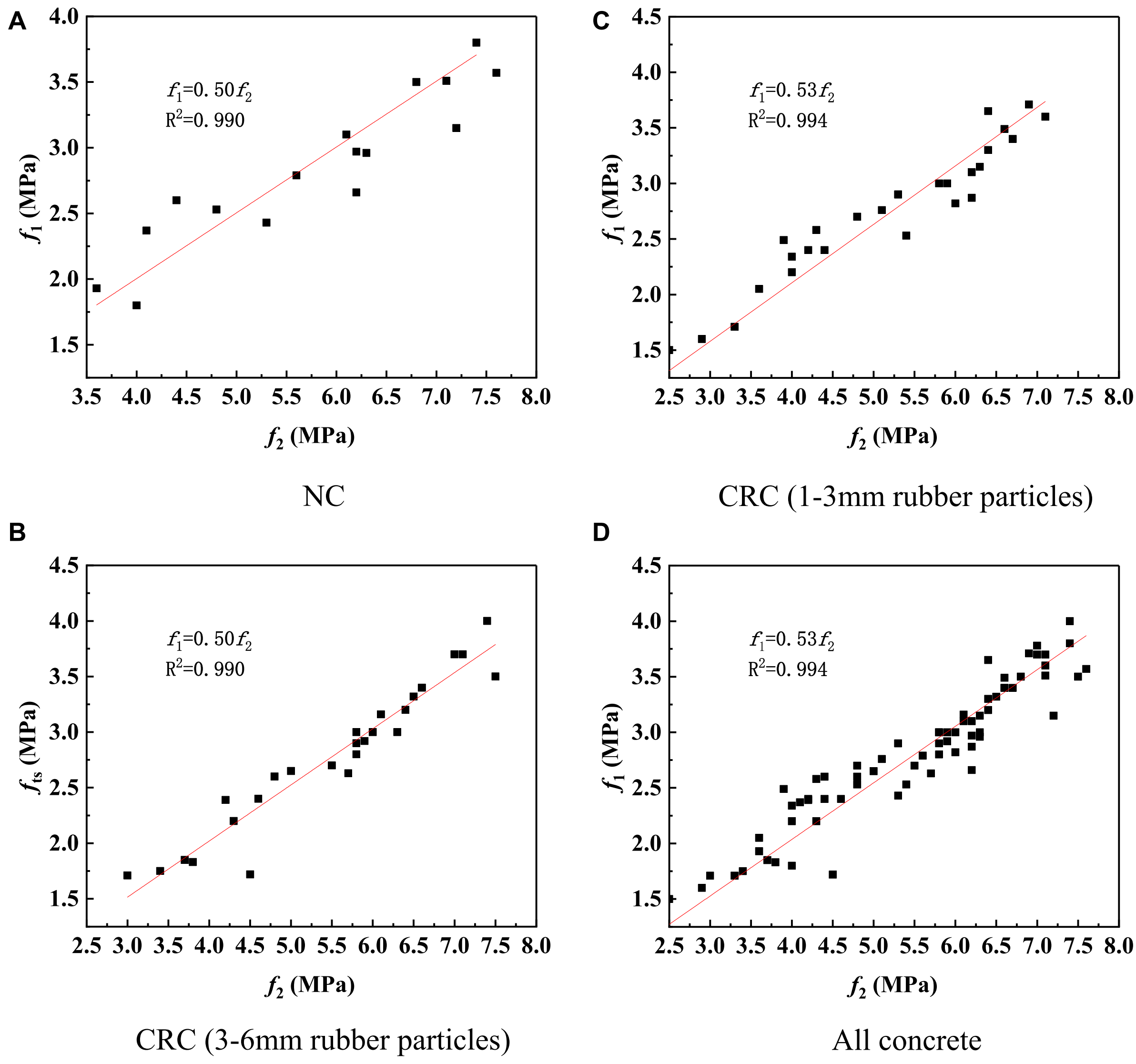

FIGURE 13
Linear fitting of Ep. (6): NC **(A)**; CRC (3–6 mm rubber particles) **(B)**; CRC (1–3 mm rubber particles) **(C)**; All concrete **(D)**.

strengths for concrete:

$$f_1 = \beta f_2' \tag{4}$$

where β is the coefficient related to the specimen size. Combined with Eq. 1 and Eq. 2, Eq. 3, Eq. 4, we obtain:

$$f_1 = \beta\gamma \frac{P_2}{A_2} = \beta\gamma f_2 \tag{5}$$

For $\psi = \beta\gamma$, the relational expression between the cube and cylinder nominal transverse splitting strength is:

$$f_1 = \psi f_2 \tag{6}$$

The linear fitting results (that pass through the origin) of Eq. 6 are shown in Figure 13. The ψ of NC (0.50; Figure 13A) differs slightly from that of the CRC (0.50 in Figure 13B, 0.53 in Figure 13C), which indicates that the incorporation of rubber particles into NC has only a small effect on ψ. The slight difference in ψ between CRC with 3–6 mm (0.50, Figure 13B) and 1–3 mm rubber particles (0.53, Figure 13C) shows that the effect of rubber particle size on ψ is small. When all of the data are combined, ψ = 0.53 with an R^2 (correlation coefficient) of 0.994 (Figure 13D).

An insertion of the value of ψ into Eq. 6 yields:

$$f_1 = 0.53 f_2 \tag{7}$$

The test value is compared to the calculated value.

The calculated f_1 values from Eq. 7 and test value f_1' are shown in Table 7. There are 17 data sets for NC and 54 data sets for CRC (27 for 3–6 mm CRC and 27 for 1–3 mm CRC) for a total of 71 data sets. Among the 71 data sets, the ratios of the calculated values f_1 to test value f_1' gives a minimum of 0.80, maximum of 1.34, mean of 0.99, and mean square error of 0.087. The ratios are relatively centralized

TABLE 7 Calculated and test splitting strengths of concrete.

Concrete	NC				3–6 mm CRC				1–3 mm CRC				f_1/f_1' Mean value	Mean square error
Sequence Number	f_2	f_1	f_1'	f_1/f_1'	f_2	f_1	f_1'	f_1/f_1'	f_2	f_1	f_1'	f_1/f_1'		
1	4.02	2.04	1.80	1.13	3.78	1.94	1.83	1.06	3.63	1.84	2.05	0.90	0.99	0.087
2	5.32	2.70	2.43	1.11	4.99	2.55	2.65	0.96	4.34	2.19	2.58	0.85		
3	5.63	2.86	2.79	1.03	5.86	3.01	2.92	1.03	5.40	2.75	2.53	1.09		
4	6.21	3.16	2.97	1.06	6.13	3.11	3.16	0.98	6.33	3.21	3.15	1.02		
5	7.19	3.67	3.15	1.17	6.51	3.32	3.32	1.00	6.42	3.26	3.65	0.89		
6	6.99	3.57	3.78	0.94	7.40	3.77	4.00	0.94	6.92	3.52	3.71	0.95		
7	3.62	1.84	1.93	0.95	4.23	2.14	2.39	0.90	3.99	2.04	2.34	0.87		
8	4.44	2.24	2.60	0.86	4.50	2.30	1.72	1.34	3.90	1.99	2.49	0.80		
9	6.07	3.11	3.10	1.00	5.72	2.91	2.63	1.11	5.10	2.60	2.76	0.94		
10	6.83	3.47	3.50	0.99	6.00	3.06	3.00	1.02	6.02	3.06	2.82	1.09		
11	7.44	3.77	3.80	0.99	7.54	3.83	3.50	1.09	6.23	3.16	2.87	1.10		
12	4.09	2.09	2.37	0.88	7.02	3.57	3.70	0.96	6.60	3.37	3.49	0.97		
13	4.80	2.45	2.53	0.97	3.73	1.89	1.85	1.02	3.32	1.68	1.71	0.98		
14	6.19	3.16	2.66	1.19	4.79	2.45	2.60	0.94	4.39	2.24	2.40	0.93		
15	6.32	3.21	2.96	1.08	5.78	2.96	3.00	0.99	5.83	2.96	3.02	0.99		
16	7.10	3.62	3.51	1.03	6.62	3.37	3.40	0.99	6.74	3.42	3.42	1.01		
17	7.60	3.88	3.57	1.09	7.10	3.62	3.70	0.98	7.08	3.62	3.61	1.01		
18					3.38	1.73	1.75	0.99	2.89	1.48	1.60	0.93		
19					4.61	2.35	2.40	0.98	4.22	2.14	2.42	0.89		
20					5.76	2.96	2.80	1.06	5.30	2.70	2.90	0.93		
21					6.42	3.26	3.20	1.02	6.18	3.16	3.13	1.02		
22					6.64	3.37	3.40	0.99	6.41	3.26	3.31	0.99		
23					3.01	1.53	1.71	0.89	2.48	1.28	1.51	0.85		
24					4.31	2.20	2.20	1.00	3.99	2.04	2.22	0.93		
25					5.54	2.81	2.70	1.04	4.82	2.45	2.71	0.91		
26					5.77	2.96	2.90	1.02	5.32	2.70	2.90	0.93		
27					6.28	3.21	3.00	1.07	5.88	3.01	3.03	1.00		

and concentrated around 1.00, as shown in Figure 14. The cube splitting strength calculated by the cylinder nominal transverse splitting strength via Eq. 7 is similar to that obtained by the cube splitting test.

4 Conclusion

The cube and cylinder nominal transverse splitting strengths of NC and CRC were determined and compared. On the basis of the results, the following conclusions can be drawn.

- The stress distribution in the tensile direction of concrete is obtained by simulating the cylinder transverse splitting test using finite element analysis software. The tensile stress distribution area of the splitting tensile failure surface is large, which is similar to the stress distribution of the cube splitting tensile failure surface. This indicates that failure during concrete cylinder transverse splitting tests is mainly determined by the tensile stress.
- The standard deviation of each group of concrete cylinder transverse splitting failure load tests is slightly lower than that obtained from the cube splitting failure load tests. This indicates a slightly higher precision of the cylinder tensile strength detected by the cylinder transverse splitting tests than that obtained by the cube splitting tensile tests.
- The cube and cylinder nominal transverse splitting strengths of NC and CRC regularly decrease with increasing water-cement

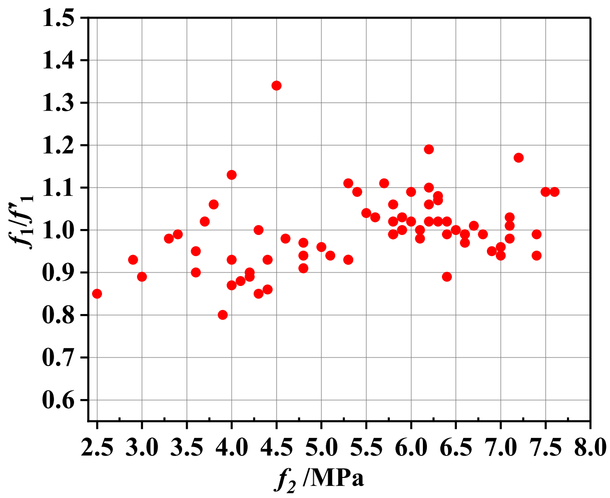

FIGURE 14
Distribution of ratio of calculated and tested cube splitting strength.

ratio and rubber content, which indicates a certain internal relationship between the cube and cylinder nominal transverse splitting strengths.

- The relationship between the cube (150 × 150 × 150 mm) and cylinder (Ø100 mm) nominal transverse splitting strength is established, $f_1 = 0.53 f_2$, with a correlation coefficient $R^2 = 0.994$. The influence of rubber particle content and particle size on ψ is small over the investigated range and can be ignored.

Data availability statement

The original contributions presented in the study are included in the article/Supplementary material, further inquiries can be directed to the corresponding author.

Author contributions

QC and SH performed material preparation, data collection, and modeling. FW performed result analysis and discussion. FW edited the manuscript. LF reviewed the manuscript. All authors contributed to the article and approved the submitted version.

Funding

The research was supported by The National Key Research and Development Program of China (2022YFC3202300), Major Science and Technology Special Projects in Henan Province (201300311400), General Science Foundation Program of Henan Province (222300420491).

Conflict of interest

The authors declare that the research was conducted in the absence of any commercial or financial relationships that could be construed as a potential conflict of interest.

Publisher's note

Supplementary material

The Supplementary Material for this article can be found online at: https://www.frontiersin.org/articles/10.3389/fmats.2023.1216747/full#supplementary-material

References

Adeboje, A. O., Kupolati, W. K., Sadiku, E. R., and Ndambuki, J. M. (2020). Characterization of modified crumb rubber concrete. *Int. J. Sustain. Dev. Plan.* 15 (3), 377–383. doi:10.18280/ijsdp.150315

Ali, N. A., Amos, A. D., and Roberts, M. (2000). Use of ground rubber tires in Portland cement concrete," in *Proc. Int. Conf. Concrete* (UK: University of Dundee), 379–390.

Benazzouk, A., Mezreb, K., Doyen, G., Goullieux, A., and Quéneudec, M. (2003). Effect of rubber aggregates on the physico-mechanical behaviour of cement–rubber composites-influence of the alveolar texture of rubber aggregates. *Cem. Concr. Comp.* 25, 711–720. doi:10.1016/s0958-9465(02)00067-7

Bhanja, S., and Sengupta, B. (2005). Influence of silica fume on the tensile strength of concrete. *Cem. Concr. Res.* 35, 743–747. doi:10.1016/j.cemconres.2004.05.024

Eldin, N. N., and Senouci, A. B. (1993). Rubber-tire particles as concrete aggregate. *J. Mater Civ. Eng.* 5, 478–496. doi:10.1061/(asce)0899-1561(1993)5:4(478)

Elsayed, M., Tayeh, B. A., Taha, Y., and El-Azim, A. A. (2022). Experimental investigation on the behaviour of crumb rubber concrete columns exposed to chloride–sulphate attack. *Structures* 46, 246–264. doi:10.1016/j.istruc.2022.10.077

Feng, W. H., Chen, Z., Tang, Y. C., Liu, F., Yang, F., Yang, Y., et al. (2022). Fracture characteristics of sustainable crumb rubber concrete under a wide range of loading rates[J]. *Constr. Build. Mater.* 359, 129474. doi:10.1016/j.conbuildmat.2022.129474

GB/T14684-2011 (2011). *Sand for construction*. China: GRA-Rock.

GB/T14685-2011 (2011). *Pebble and crushed stone for construction*. China: GRA-Rock.

GB/T50081-2002 (2002). *Standard for test method of mechanical properties on ordinaty concrete*. China: Ministry of Construction of the People's Republic of China.

Ge, W., Jiao, Y., Wu, M., Li, Z., Wang, T., Li, W., et al. (2022). Estimating loss of life caused by dam breaches based on the simulation of floods routing and evacuation potential of population at risk. *J. Hydrology* 612, 128059. doi:10.1016/j.jhydrol.2022.128059

Ge, W., Qin, Y., Li, Z., Zhang, H., Gao, W., Guo, X., et al. (2020). An innovative methodology for establishing societal life risk criteria for dams: A case study to reservoir dam failure events in China. *Int. J. Disaster Risk Reduct.* 49, 101663. doi:10.1016/j.ijdrr.2020.101663

Haldar, P., and Karmakar, S. (2021). An experimental study on the fatigue properties of Alccofine-based crumb rubber concrete. *Proc. Institution Civ. Eng. Eng. Sustain.* 174 (5), 235–250. doi:10.1680/jensu.20.00080

Han, T. H., Ji, J. H., Dong, Z. Q., Zhu, H., and Wu, G. (2023). Compression behavior of concrete columns strengthened by a hybrid BFRP/HDPE tube coupled with a crumb rubber concrete cladding layer[J]. *Constr. Build. Mater.* 364, 129969. doi:10.1016/j.conbuildmat.2022.129969

Hang, J. F., and Fan, K. (2011). Abrasion resistance of rubberized concrete. *J. Tianjin Univ.* 44, 727–731. doi:10.3969/j.issn.0493-2137.2011.08.012

Hernandez, Q. F., Barluenga, G., and Bollati, M. (2002). Static and dynamic behaviour of recycled tyre rubbe-filled concrete. *Cem. Concr. Res.* 32, 1587–1596. doi:10.1016/S0008-8846(02)00833-5

JGJ/T384-2016 (2016). *Technical specification for testing concrete strength with drilled core method*. China: Wiley.

Jia, F. (1997). Experimental research on the test of the compressive strength of the heated concrete with small diameter cores of 45mm and 70mm by transverse cutting method. *J. Northwest Ins. Archit. Eng.* 1, 8–11. doi:10.13204/j.gyjz199606012

Kanos, A., Giannakopoulis, A. E., and Perdikaria, P. C. (2006). "Size effect on concrete splitting tensile strength and modulus of elasticity," in *Measuring, monitoring and modeling concrete properties* (Netherlands: Springer).

Khan, I., Shahzada, K., Bibi, T., Ahmed, A., and Ullah, H. (2021). Seismic performance evaluation of crumb rubber concrete frame structure using shake table test. *J. Struct.* 30, 41–49. doi:10.1016/j.istruc.2021.01.003

Li, Z., Zhang, Y., Wang, J., Ge, W., Li, W., Song, H., et al. (2021). Impact evaluation of geomorphic changes caused by extreme floods on inundation area considering geomorphic variations and land use types. *Sci. Total Environ.* 754, 142424. doi:10.1016/j.scitotenv.2020.142424

Lin, Q., Liu, Z. Q., Sun, J. L., and Yu, L. (2023). Comprehensive modification of emulsified asphalt on improving mechanical properties of crumb rubber concrete[J]. *Constr. Build. Mater.* 369, 130555. doi:10.1016/j.conbuildmat.2023.130555

Lu, Y. B., and Li, Q. M. (2011). About the dynamic uniaxial tensile strength of concrete-like materials. *Int. J. Impact Eng.* 38, 171–180. doi:10.1016/j.ijimpeng.2010.10.028

Malhotra, V. M. (1970). Effect of specimen size on tensile strength of concrete. *ACI J.* 67, 1. doi:10.14359/7292

Mindess, S., Young, J. F., and Darwin, D. (2002). *Concrete*. 2nd Ed. Upper Saddle River (USA): Pearson Education, Inc.

Nilsson, S. (1961). The tensile strength of concrete determined by splitting tests on cubes. *RILEM Bulletin* 11, 63–67.

Olesen, J. F., Ostergaard, L., and Stang, H. (2006). Nonlinear fracture mechanics and plasticity of the split cylinder test. *Mater Struct.* 39, 421–432. doi:10.1617/s11527-005-9018-3

Paine, K. A., and Dhir, R. K. (2002). Kopasakis. Use of crumb rubber to achieve freeze thaw resisting concrete," in *Proceedings of the international conference concrete for extreme conditions (ICE)* (London, United Kingdom: Thomas Telford Limited), 485–498.

Raphael, J. M. (1984). Tensile strength of concrete. *J. Am. Concr. Institution* 81, 158–165. doi:10.14359/10653

Rashid, M. A., Mansur, M. A., and Paramasivam, P . (2002). Correlations between mechanical properties of high-strength concrete. *J. Mater Civ. Eng.* 14 (3), 230–238. doi:10.1061/(asce)0899-1561(2002)14:3(230)

Rocco, C., Guinea, G. V., Planas, J., and Elices, M. (2000). Review of the splitting-test standards from a fracture mechanics point of view. *Cem. Concr. Res.* 31, 73–82. doi:10.1016/s0008-8846(00)00425-7

Sarfarazi, V., Haeri, H., Ebneabbasi, P., Shemirani, A. B., and Hedayat, A. (2018). Determination of tensile strength of concrete using a novel apparatus. *Constr. Build. Mater* 166, 817–832. doi:10.1016/j.conbuildmat.2018.01.157

Savas, B. Z., Ahmad, S., and Fedroff, D. (1997). Freeze-thaw durability of concrete with ground waste tire rubber. *Transp. Res. Rec.* 1574, 80–88. doi:10.3141/1574-11

Segre, N., and Jocke, L. (2000). Use of tire rubber particles as addition to cement paste. *Cem. Concr. Res.* 30, 1421–1425. doi:10.1016/s0008-8846(00)00373-2

Segre, N., Monteiro, P. J. M., and Sposito, G . (2002). Surface characterization of recycled tire rubber to be used in cement paste matrix. *Colloid Interfac Sci* 248, 521–523. doi:10.1006/jcis.2002.8217

SL352-2006 (2006). *Test code for hydraulic concrete*. China: Reaffirmed.

Sun, J. J., Chen, X., Fu, Z. W., and Lacidogna, G. (2021). Damage pattern recognition and crack propagation prediction for crumb rubber concrete based on acoustic emission techniques. *Appl. Sci.* 11 (23), 11476. doi:10.3390/app112311476

Swaddiwudhipong, S., Lu, H. R., and Wee, T. H. (2003). Direct tension test and tensile strain capacity of concrete at early age. *Cem. Concr. Res.* 33 (12), 2077–2084. doi:10.1016/s0008-8846(03)00231-x

Tang, T. (1994). Effects of load-distribute width on split tension of unnotched and notched cylindrical specimens. *J. Test. Eval.* 22, 401–409. doi:10.1520/JTE12656J

Topcu, I. B., and Avcular, N. (1997). Collision behaviours of rubberized concrete. *Cem. Concr. Res.* 27, 1893–1898. doi:10.1016/s0008-8846(97)00204-4

Topcu, I. B. (1995). The properties of rubberized concretes. *Cem. Concr. Res.* 25, 304–310. doi:10.1016/0008-8846(95)00014-3

Toutanji, H. A. (1996). The use of rubber tire particles in concrete to replace mineral aggregates. *Cem. Concr. Comp.* 18, 135–139. doi:10.1016/0958-9465(95)00010-0

Wang, T., Li, Z., Ge, W., Zhang, H., Zhang, Y., Sun, H., et al. (2023). Risk consequence assessment of dam breach in cascade reservoirs considering risk transmission and superposition. *Energy* 265, 126315. doi:10.1016/j.energy.2022.126315

Wang, T., Li, Z., Ge, W., Zhang, Y., Jiao, Y., Sun, H., et al. (2022). Calculation of dam risk probability of cascade reservoirs considering risk transmission and superposition. *J. Hydrology* 609, 127768. doi:10.1016/j.jhydrol.2022.127768

Wu, M., Wu, Z., Ge, W., Wang, H., Shen, Y., and Jiang, M. (2021). Identification of sensitivity indicators of urban rainstorm flood disasters: A case study in China. *J. Hydrology* 599, 126393. doi:10.1016/j.jhydrol.2021.126393

Wu, S., Chen, X., and Zhou, J. (2012). Tensile strength of concrete under static and intermediate strain rates: Correlated results from different testing methods. *Nucl. Eng. Des.* 250, 173–183. doi:10.1016/j.nucengdes.2012.05.004

Xiao, F., Yu, J., and Lu, Z. (2011). Experimental study on the test of multiple transverse splitting method of concrete core sample. Low. *Temp. Build. Technol.* 3, 40–42.

Xu, J., Niu, X. L., Yao, Z. Y., Wang, M., Wang, L., Li, J., et al. (2021). Rapid identification of plasmid replicon type and coexisting plasmid-borne antimicrobial resistance genes by S1-pulsed-field gel electrophoresis-droplet digital polymerase chain reaction. *Constr. Build. Mater.* 18, 298–305. doi:10.1089/fpd.2020.2865

Xu, X. Q., Zhang, Z. G., Hu, Y. G., and Wang, X. (2020). Bearing strength of crumb rubber concrete under partial area loading. *J. Mater.* 13 (11), 2446. doi:10.3390/ma13112446

Yang, Z. M., and Li, N. P. (2002). Application of small diameter core sample to the compressive strength identification of concrete structure. *J Xi'an Univ Archit Tech* 34, 407–409. doi:10.3969/j.issn.1006-7930.2002.04.026

Youssf, O., Swilam, A., and Tahwia, A. M. (2023). Performance of crumb rubber concrete made with high contents of heat pre-treated rubber and magnetized water[J]. *J. Mater. Res. Technol.* 23, 2160–2176. doi:10.1016/j.jmrt.2023.01.146

Yu, J., Jiang, J., and Lu, Z. (2010). One suggestion on the coredrilling method of concrete testing:several times oftransverse cutting. *Sichuan Buiding Sci.* 36 (1), 84–87.

Yuan, Q., Du, W. B., Li, Z. K., and Li, S. (2006). Research on the test of the tensile strength of concrete cylinder by transverse cutting method. *Ind. Constr.* 36, 83–87. doi:10.13204/j.gyjz200606023

Yuan, Q., Li, L. Q., and Lu, Y. (2016). Extension and application of transverse cutting method for tensile strength measurement of concrete. *J. Hydro Eng.* 1, 125–135. doi:10.11660/slfdxb.20160116

Zhang, H., Ge, W., Zhang, Y., Li, Z., Li, W., Zhu, J., et al. (2023). Risk management decision of reservoir dams based on the improved life quality index. *Water Resour. Manag.* 37, 1223–1239. doi:10.1007/s11269-023-03426-y

Zhou, H., Che, Y., and Chen, G. (2008). Size effect on tensile splitting strength of concrete cubes and cylinders. *Concrete* 8, 13–16. doi:10.3969/j.issn.1002-3550.2010.08.005

Zi, G., Oh, H., and Park, S. K. (2008). A novel indirect tensile test method to measure the biaxial tensile strength of concretes and other quasibrittle materials. *Cem. Concr. Res.* 38 (6), 751–756. doi:10.1016/j.cemconres.2008.02.002